Collaborative simulations and experiments for a novel yield model of coal devolatilization in oxy-coal combustion conditions

Salvatore Iavarone[a,b,*], Sean T. Smith[c], Philip J. Smith[c], Alessandro Parente[a,b,**]

[a] *Université Libre de Bruxelles, Ecole Polytechnique de Bruxelles, Aero-Thermo-Mechanics Laboratory, Bruxelles, Belgium*
[b] *Université Libre de Bruxelles and Vrije Universiteit Brussel, Combustion and Robust Optimization Group (BURN), Bruxelles, Belgium*
[c] *University of Utah, Department of Chemical Engineering, Salt Lake City, UT, 84112, USA*

Abstract

Oxy-coal combustion is an emerging low-cost "clean coal" technology for emissions reduction and Carbon Capture and Sequestration (CCS). The use of Computational Fluid Dynamics (CFD) tools is crucial for the development of cost-effective oxy-fuel technologies and the minimization of environmental concerns at industrial scale. The coupling of detailed chemistry models and CFD simulations is still challenging, especially for large-scale plants, because of the high computational efforts required. The development of scale-bridging models is therefore necessary, to find a good compromise between computational efforts and the physical-chemical modeling precision. This work presents a procedure for scale-bridging modeling of coal devolatilization, in the presence of experimental error, that puts emphasis on the thermodynamic aspect of devolatilization, namely the final volatile yield of coal, rather than kinetics. The procedure consists of an engineering approach based on dataset consistency and Bayesian methodology including Gaussian-Process Regression (GPR).

Experimental data from devolatilization tests carried out in an oxy-coal entrained flow reactor were considered and CFD simulations of the reactor were performed. Jointly evaluating data and simulations, a novel yield model was validated against the data via consistency analysis. In parallel, a Gaussian-Process Regression was performed, to improve the understanding of the uncertainty associated to the devolatilization, based on the experimental measurements. Potential model forms that could predict yield during devolatilization were obtained. The set of model forms obtained via GPR includes the yield model that was proven to be consistent with the data. The overall procedure has resulted in a novel yield model for coal devolatilization and in a valuable evaluation of uncertainty in the data, in the model form, and in the model parameters.

Keywords: Coal devolatilization; Consistency analysis; Gaussian-Process Regression; Oxy-coal combustion; Yield model.

1. Introduction

Fossil fuels are expected to continue supplying much of the energy used worldwide. Among them, coal shows the most important growth in demand and it will still account for 30% of the overall electricity generated in 2030 [1]. To reduce the environmental concerns linked to the use of coal, oxy-combustion technologies are of intense industrial

*Correspondence to: S. Iavarone, Avenue F.D. Roosevelt 50, 1050 Bruxelles, Belgium.
**Correspondence to: A. Parente, Avenue F.D. Roosevelt 50, 1050 Bruxelles, Belgium. Phone: +3226502680
Email addresses: Salvatore.Iavarone@ulb.ac.be (Salvatore Iavarone), Alessandro.Parente@ulb.ac.be (Alessandro Parente)

interest [2]. The use of simulation tools such as computational fluid dynamics (CFD) appears necessary to allow the development of cost-effective oxy-coal technologies at a scale sufficient to augment existing energy options. CFD calculations can be applied directly at the industrial scale of interest, thus avoiding scaling-up the results from lab-scale experiments. However, this advantage can only be obtained if CFD calculations are quantitatively predictive and are trusted as so. Despite the improvements in the computational capability, the coupling of detailed chemistry models and CFD simulation can still be prohibitive for real combustors, which require large computational grids. In these cases, the development of scale-bridging models, namely reduced physics model with quantified model-form uncertainty to bridge scales from a more complex physics model, is necessary. Since devolatilization is the first step in thermochemical processes involving solid fuels that influences the overall subsequent reactions, comprehensive CFD codes for the study and optimization of coal combustion in lab, pilot and industrial-scale plants, demand a proper devolatilization model [3–5].

Devolatilization processes can be viewed from a kinetic or thermodynamic perspective. A comprehensive devolatilization model must be capable of capturing thermodynamic characteristic, i.e. the ultimate volatile yield of the coal, and the kinetics of how the coal reaches its ultimate yield. In industrial applications, kinetics occurs with widely varied time scales and within a minimal region of the whole domain: *the amount* of material transferred to the gas phase is judged to be more influential within the application than *the rate* at which this occurs. Hence, for this type of applications, thermodynamic effects should be primarily considered. Devolatilization modeling has focused mostly on kinetics: the available models range from simple approaches, such as single, parallel, distributed kinetic or multistep models [6–9], to complex structural phenomenological models, such as FLASH-CHAIN, CPD and FG-DVC [10–12]. The simple approaches are applied to specific coals and operating ranges, and they must be tuned to the right range of temperatures, heating rates and residence times. The phenomenological models are fundamental and more reliable, but computationally expensive, even though the CPD model was recently employed in flamelet LES modeling of coal combustion [13].

The ultimate/steady-state/equilibrium yield can always be obtained from a kinetic model, but obtaining accurate yields from kinetics requires resolution of all time scales in the kinetic mechanism. An explicit equilibrium-yield model avoids the need to accurately integrate through these fast time scales and is therefore highly desirable for a CFD application. Thus, the development of a yield model, with an explicit functional form and parameters derived through a collaboration of experiments and numerical simulations, is attractive.

A first attempt to develop a comprehensive yield model, needed to improve the predictivity of simple models when experimental data are not available, was proposed by Biagini and Tognotti [14]. Their approach aimed to improve the simplest kinetic model, i.e. the Single First-Order Reaction model [15], whose approximation is not generally accepted [16–18], but widely used, due to simplicity and somehow sufficient accuracy [19–22]. The main drawback of the SFOR model is the assumption of a constant ultimate volatile yield, equal to the value from the proximate analysis. To overcome this drawback, Biagini and Tognotti proposed a yield model, i.e. a simple functional form that relates the ultimate volatile yield to the particle temperature, referred to here as BT model. The BT model was tested in our previous work [23] against an experimental dataset collected in a pilot-scale entrained flow reactor (EFR) and led to a non-optimal prediction of the coal yield. The model parameters, which were not tuned on the operating conditions and the coal type of interest, were considered accountable for the poor performances of the BT

model.

The present work is a follow-on to the results obtained and showed in [23], which emphasized the sensitivity of first-order kinetic models to the value of the ultimate volatile yield. Therefore, the modeling of the ultimate yield has been targeted and performed, using two approaches that allow the collaborative analysis of experiments and simulations: consistency analysis [24] and a Bayesian method based on Gaussian-Process Regression [25]. The development of the yield model progressed in the following three steps: first, the model form for ultimate yield proposed by Biagini and Tognotti as well as alternative naive forms were compared directly to the experimental data and were shown to be inconsistent by the metric described below. Second, a non-parametric statistical method, unconstrained to a specific model form, was used to indicate the ultimate yield empirically. Third, a new model form was proposed and demonstrated to be consistent with the experimental data.

2. Experimental data

Validation of reduced models relies on experimental data. For coal combustion the most common experiments have historically been thermogravimetric analysis (TGA) and drop tube reactor (DTR) experiments [26–28], although recently the entrained flow reactors (EFR) are emerging as a more viable tool for derivation, validation and uncertainty quantification of models in conditions similar to those of industrial-scale facilities [29–31]. The experimental data used in this work are the results of devolatilization tests carried out in the same experimental apparatus, the Isothermal Plug Flow Reactor (IPFR), at 1173, 1373 and 1573 K, and performed on the Sebuku bituminous coal. The data, along with the results of other experiments performed in the same facility (devolatilization, char oxidation, nitrogen partitioning etc.), can be found in [32]. Table 1 reports the particle size and proximate analysis data of Sebuku coal.

Coal type	Particle size (μm)	Proximate Analysis (%wt dry)			Ultimate Analysis (%wt dry)				
		VM	FC	Ash	C	H	N	S	O
Sebuku	65-90	40.30	47.95	11.75	62.75	4.66	1.27	0.48	19.10

Table 1: Sebuku coal characteristic properties.

The IPFR is an EFR operated by the International Flame Research Foundation (IFRF) and it allows severe thermal conditions to be reached, i.e. high temperatures (up to 1600 K) and heating rates (circa 10^4–10^5 K/s). It is mainly composed of three parts: a gas pre-heating 60 kW burner, a vertical isothermal reactor, and an exhaust line. In addition to these sections, it includes a coal feeder and a water-cooling system. The vertical reactor is a drop tube (4.5 m total length $\times$ 0.15 m inner diameter) consisting of nine modules equipped with a 54 kW heating system, i.e. silicon carbide U-type heating elements, located at the walls, to ensure isothermal conditions within a margin of 10-20 K along the tube [33–35]. Pulverized fuel particles are injected from a side through a radial probe and transported by a carrier gas (nitrogen/air/carbon dioxide) into a flue-gas stream, coming from the preheating combustion section located at the top (see Fig. 1). The material is sieved and samples of size fractions in the range 65–90 μm are studied. The solid flow rate is up to 100 g/h, while the flow rates of the carrier CO_2 stream and of the flue gases are 0.5-0.6 Nm^3/h and 14.6-17.6 Nm^3/h, respectively [36].

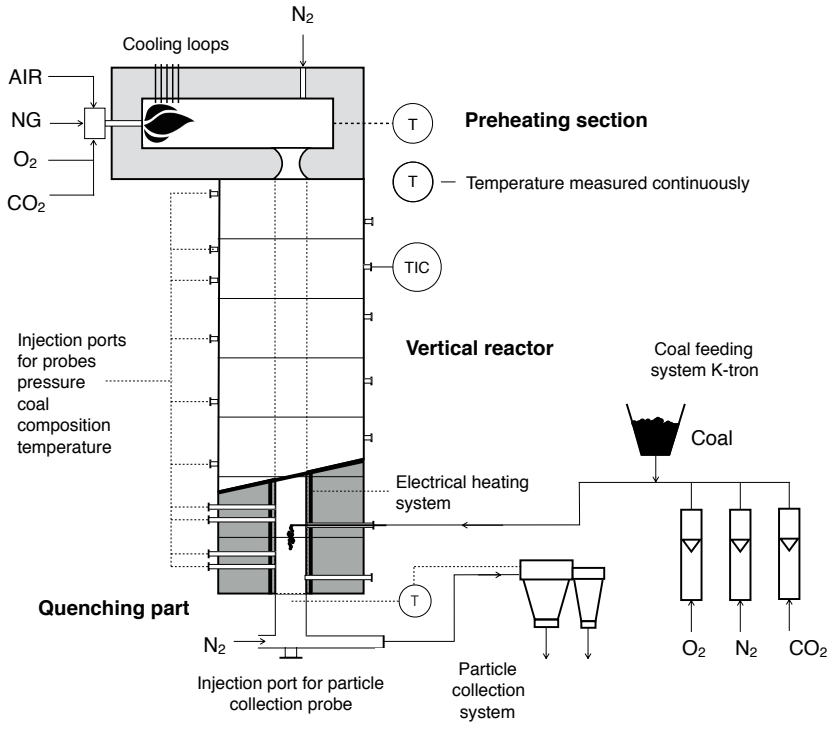

Figure 1: Scheme of Isothermal Plug Flow Reactor.

The devolatilization tests examined in this paper are the same considered in our previous work [23] where the details of the gas composition in each experiment can be found, along with a discussion on the negligible influence of oxidation and gasification reactions.

The solid residue and gaseous products are quenched and sampled in the collection probe for online and offline analyses: proximate, ultimate, ash composition and particle size distribution. From the results of the proximate analyses, expressed in dry basis, the conversion value for each sample is calculated according to the ash tracer method: the ash matter is supposed to remain constant during the devolatilization process, and the ash content of the solid residue is then compared to that of the parent coal for calculating the conversion X, as

$$X = 1 - ash_0/ash \times (1 - ash)/(1 - ash_0), \tag{1}$$

where ash_0 and ash are initial and current ash mass fraction respectively [35]. Each experimental result is defined by a value of the nominal particle residence time, the nominal reactor temperature and the devolatilization conversion. In particular, the results are reported for five residence times at each nominal reactor temperature. The particles residence time is calculated from the length of the particles path within the vertical reactor, i.e. the distance between injection and sampling height, and the mean velocity of the flue gases. The assumption of nominal reactor temperature uniformly and quickly reached by the particles is made by the experimenters, therefore measurements of the solid phase temperature were not performed. The flue gases reach the nominal temperature within the preheating section, whereas the carrier stream enters the reactor at 293 K. The carrier gas flow rate is almost thirty times lower than the coflow rate, so that a small influence on the particle heating rate and temperature is expected.

The experimental error on the conversion values was estimated and reported by the experimenters. Accordingly,

a 4% relative error was found to affect the conversion value almost constantly regardless of the temperature. The composition of ash, the inhomogeneity of the collected sample and the accuracy of the proximate analyser were considered as potential sources of uncertainty [37]. Both a CFD and a statistical analysis pointed out that the experimental uncertainty is larger than the estimated 4%, as it will be shown in Section 5. In particular, a joint experimental and numerical analysis was carried out: CFD simulations were used to help assess the different sources of uncertainty and to better evaluate the overall experimental error.

3. Numerical settings

The ultimate volatile yield depends on the thermal history of the coal during the devolatilization [16, 38, 39]. Since the lack of experimental measurements of the particle temperature, the effective particle thermal history is estimated from a CFD model, used as a diagnostic tool. This approach is important to avoid the rough assumption that the particle temperature is constant during the devolatilization test, and thus accounting for the heat transfer in the actual conditions. The simulations used a two-way coupled Lagrangian tracking and were developed using Ansys Fluent 16. The domain consisted of half IPFR because of its geometric symmetry. The chosen domain referred to the setting with the larger reactor length, i.e. larger distance between feeding piper and sampling probe, to avoid creating one mesh for each experimental run. A grid independency study on the velocity field was performed and a grid consisting of about 0.9 million of cells was chosen. The nominal reactor temperature was set to three different values, i.e. 1173 K, 1373 K and 1573 K, while the temperature of injected particles was set to 293 K in all the cases. The boundary conditions were taken directly from the experiments. The particle size distribution was of Rosin-Rammler type, going from 65 to 90 μm. The dispersion of particles due to turbulence in the fluid phase was predicted using the stochastic tracking model, which includes the effect of instantaneous turbulent velocity fluctuations on the particle trajectories through the Discrete Random Walk (DRW) method. In addition to turbulent dispersion, drag and gravity were considered to be the forces acting on the particles. RANS equations were solved using the standard k-ε turbulence model and the Eddy Dissipation Model was used to treat the turbulence-chemistry interactions of the gaseous phase. Radiation was taken into account using the P1 radiation model, in combination with the Weighted Sum of Gray Gases Model (WSGG) for spectral properties. The particle emissivity was set to 0.7. A stationary solver was used, with a second order discretization scheme and the SIMPLE algorithm for pressure-velocity coupling. The considered devolatilization models were implemented via User Defined Functions (UDFs). The models and methods discussed are considered to be standard to a coal combustion simulation as a compromise between accuracy, reliability, and simulation time.

4. Preliminary CFD simulations

The CFD modeling was performed at different levels of complexity, to gain insight into specific flow features. Part of the results of the CFD modeling of the IPFR can be found in [23]. Histograms of the particle temperature distributions from the inert CFD simulations are shown in Fig. 2 for the three experimental cases. The different colors account for the five different sampling points. The numerical results show that uncertainties in particle temperature are greater than those on the yields (4% relative error) during the early stages of heating, but diminish throughout and

ultimately vanish. The particles do not reach the nominal reactor temperature uniformly and instantaneously. One may conclude that the uncertainties on the volatiles yields are not only due to sampling and analytical procedures, as pointed out during the experimental campaign, but also to the particle thermal histories inside the reactor.

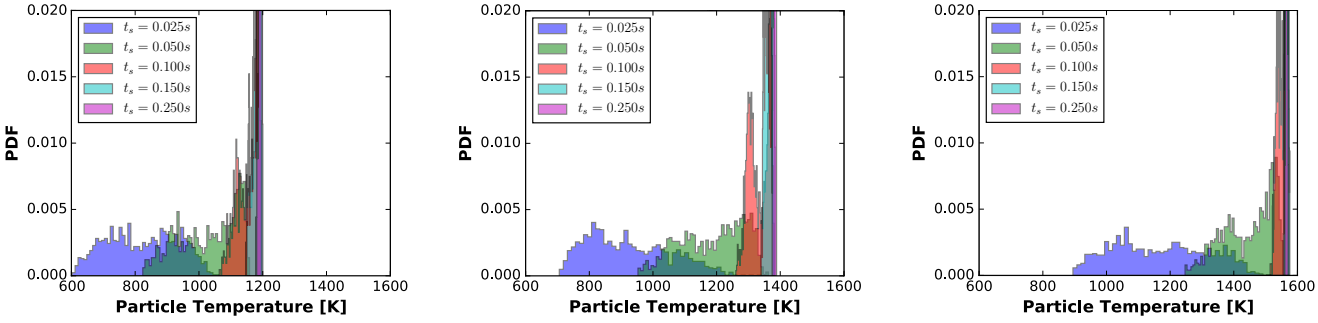

(a) (b) (c)

Figure 2: PDF of particle temperatures for inert CFD simulations at 1173 K (a), 1373 K (b) and 1573 K (c). Different colors account for the five experimental sampling times t_s.

The analysis of the particle thermal history suggested that while at the lowest temperatures the assumption of a kinetically-limited process can be made, at the highest temperatures this assumption can likely be biased, particularly for the last sampled points. In these cases, the particle residence times are comparable with the equilibrium time scales of devolatilization and the conversion values can be considered ultimate-yield values. Thus, the experimental data considered in this work are suitable for the validation of a yield model that can predict the dependence of the ultimate volatile yield on the hold temperature, i.e. the temperature at which the chemical equilibrium is reached. A yield model is strongly needed in simple kinetic approaches, which are highly desirable in CFD simulations of real combustors, but are often characterised by poor predictivity, since they estimate the same final conversion value under different thermal conditions. A recent simple model, which embodies an ultimate yield function of the particle temperature, is the one proposed by Biagini and Tognotti [14]. The BT model is a modification of the Single First-Order Reaction (SFOR) model, which assumes that devolatilization occurs in a single step according to a first-order law:

$$\frac{dX}{dt} = A \exp\left(-\frac{\mathrm{E}}{RT_p}\right)(X_f - X). \tag{2}$$

In Eq. 2, X is the volatile yield, or particle conversion, t is the time, R is the ideal gas constant and T_p is the particle temperature. It requires two kinetic parameters, i.e. the pre-exponential factor A and the activation energy E of an "artificial" first-order kinetic rate expression, and the final volatile matter yield X_f. Biagini et al. [14] proposed a model where the ultimate volatile yield is a function of temperature:

$$X_f = 1 - \exp\left(-DI\frac{T_p}{T_{st}}\right). \tag{3}$$

In Eq. 3, DI is the so-called Devolatilization Index, a dimensionless parameter specific for each coal, T_p is the particle temperature and T_{st} is the temperature from the proximate analysis. The total number of parameters in this approach is still three, as in the original SFOR model. In addition to the above-mentioned drawback of considering a constant ultimate volatile yield, equal to the value from the proximate analysis, another drawback of the SFOR

model can be considered the absence of any dependence whatsoever between the volatile yield and particle size, whose importance has been pointed out by other works, e.g., by Hashimoto et al. [40]. The size dependence would introduce more uncertainty in the particle conversion, because the general tendency for greater yields from smaller particles (yield enhancement due to faster heating rates) is compounded by large variations among the thermal histories of particles in different regions of the flow cross section. In the BT approach, the temperature is considered the principal state-space variable for both the chemical kinetics and the steady-state/equilibrium volatile yield, and the effective thermal history of the particle is considered and derived from a CFD analysis: the particle size affects the heating rate and so the particle temperature, which in turn affects the kinetic rate and ultimate yield. The size dependence is so implicitly taken into account. This approach has been followed, although alternative contexts [40] may be equally viable.

Linear correlations between coal properties and devolatilization kinetic parameters in a range of coal compositions and operating conditions have been proposed by Biagini et al., having the following general form:

$$P = mV + q, \tag{4}$$

where P is a model parameter (A, E or DI), V is a fuel parameter and m and q are the determined correlation parameters. The parameters were derived through an optimization procedure applied to a specific devolatilization data set extracted from the Solid Fuel DataBase (SFDB) of the IFRF [41]. Biagini and Tognotti verified that the best linear regressions (i.e., with the highest value of squared Pearson coefficient R^2) are for DI with VM (Volatile Matter from the proximate analysis), E with O/C (Oxygen-to-Carbon mass ratio), and $\ln(A)$ with E, even though E is not a fuel parameter *per se*. The values of m and q and the specification of model and fuel parameters are reported in Table 2.

P	V	m	q
E (kJ/mol)	O/C	30.4	24.6
ln(A) with A in (s^{-1})	E (kJ/mol)	0.105	3.42
DI	VM (%wt dry)	0.0219	-0.208

Table 2: Parameters for the generalized correlations in Equation 4.

The computed model parameters, specific for Sebuku coal, are $E = 33.9\ kJ/mol$, $A = 1068.6\, s^{-1}$ and $DI = 0.675$. The BT model was implemented in Fluent and CFD simulations of the IPFR were performed at the three nominal temperatures. The results are reported in Fig. 3. Particle conversion distributions are obtained for each sampling point. A large variance of these distributions was observed, due to the very different histories, thermal and dynamic, that each particle follows in the system. Moreover, they appear to be skewed and so might be improperly described by considering mean and standard deviation. Hence, a boxplot of the modeled conversion can give more useful information. On each box, the dot is the mean, the central line is the median, the edges of the box are the 25^{th} and 75^{th} percentiles, the whiskers extend to the most extreme data points not considered outliers, and outliers are plotted individually as crosses. Points are drawn as outliers if they are larger than $q_3 + w(q_3 - q_1)$ or smaller than $q_1 - w(q_3 - q_1)$, where q_1 and q_3 are the 25^{th} and 75^{th} percentiles, respectively, and w is equal to 1.5, corresponding

to approximately $\pm 2.7\sigma$ and 99.3 for normally distributed data. Figure 3 shows the experimental data along with uncertainty quantified by the methods that will be described in the following Section 5 (black bars), and boxplot of numerical results for the particle conversion, or yield, X over residence time t, at the three different temperatures. The predictions of BT model do not match the experimental values particularly at temperature lower than about 1300 K. The performances of the BT model can be related to its yield model parameters, which are not trained on the specific coal subject of investigation, as already discussed in [23]. A procedure for the updating of these parameters, based on a joint analysis of experimental data and CFD simulations, is then required.

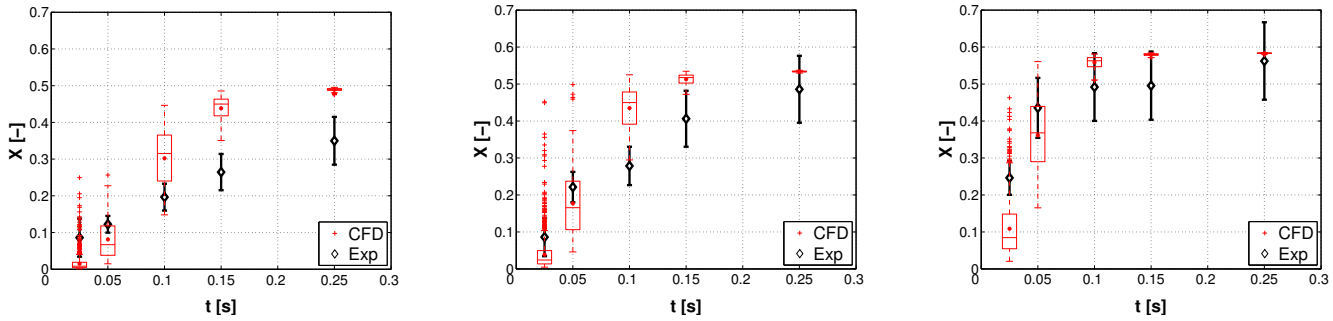

(a) (b) (c)

Figure 3: Boxplots of particle conversions vs. residence times for BT model at 1173 K (a), 1373 K (b) and 1573 K (c).

5. Model construction procedure

Two methods have been followed to assess the experimental observations, to tweak an existent yield model and to eventually construct a new yield model: a numerical approach of data collaboration, i.e. consistency analysis, and a math-based approach, i.e. the Bayesian Gaussian-Process Regression. Details of the two approaches are reported in the following subsections.

5.1. Consistency analysis

The idea of a consistent space comes from the methodology described within Feeley et al. [24], where it was used to calibrate parameter values for the methane combustion reaction-set, GRI-Mech 3.0. The basic premise of a consistent space can be described by the Eq. 5.

$$(1-\gamma)l_i \leq M_i(\mathbf{x}) - d_i \leq (1-\gamma)u_i \quad \text{for } i = 1, ..., N_{QoI}. \tag{5}$$

The model outputs M at specified parameter inputs $\mathbf{x}$ are compared directly to experimental data d, for a selected quantity of interest, QoI, having u and l as upper and lower error bounds, respectively. The uncertainty in the QoI quantified by the uncertainty exploration acts as the error bounds, that could be enlarged or reduced by means of the term γ. In this case, the only quantity of interest is the yield and the parameter inputs are DI and T_{st}. The calculation of model outputs requires the particle temperature, taken from CFD simulations for each experimental scenario, sampling point and coal parcel. The comparison between model and experiments proves consistency for the QoI if the bias is within the upper and lower error bounds of the data. This model consistency or inconsistency

can be further characterized by the term γ, i.e. the decimal fraction by which the error bounds could be either shrunk while maintaining consistency or expanded to reach consistency. The prior parameter space, or hypercube, is specified as:

$$\alpha_j \leq x_j \leq \beta_j \quad \text{for } j = 1, ..., n \ , \tag{6}$$

where α and β designate the prior bounds for each parameter x_j. If model consistency is found, the posterior parameter space will correspond to a subspace of the parameter's prior hypercube. If no consistent region is located, then the hypercube's prior bounds as well as the experimental error bounds could be re-evaluated for possible expansion.

A first attempt to determine an optimal yield model with respect to the available experimental data was carried out changing the parameters of the BT yield function, namely DI and T_{st}, to find consistency amongst the whole dataset. No global consistency was nevertheless found using the BT model, even when increasing artificially the experimental relative error to 50%. The results are shown in Section 6. Given the inconsistency of the BT model, the selection of an alternative, consistent, model form was made, following the approach of data collaboration [42, 43]. Data collaboration means transferring the uncertainties of the "raw" (experimental) data into the model directly. Doing so allows one to harvest substantially more of the information content of the data and determine more-realistic bounds on model predictions [24].

In addition to the BT model, different model forms were initially attempted and have been proved inconsistent. After obtaining results from the Gaussian-process regression (described in the next section) a new model form was easily identified , shown in Eq. 7:

$$X_f = 0.5 \times \left[1 + \text{erf}\left(\frac{T_p - T_1}{T_2\sqrt{2}}\right)\right], \tag{7}$$

and this form did prove to be consistent with the experimental data. This model form contains only two parameters, T_1 and T_2, the same number as in the BT model, and its codomain is equal to the interval [0,1], namely all the possible values of coal conversion. The error function is not uncommon in the devolatilization modeling, as it appears in the resolution (integration) of the exponential term arising in the Distributed Activation Energy Model (DAEM), when a Gaussian distribution of activation energies is taken into account [44]. Accordingly, the proposed model form can be loosely explained by the fact that the volatile yield is still an exponential function of the particle temperature, like Biagini and Tognotti suggested, and the particle temperatures are distributed according to a Gaussian centered around T_1 and having a width designated by T_2. The consistency analysis was performed to find the posterior space of the parameters T_1 and T_2. The results of analysis are shown and discussed in Section 6.

5.2. Gaussian-Process Regression

It is expected that most readers of this article have interest in coal process modeling rather than application of recent statistical tools. As such this sub-section will start with a brief overview of Gaussian-Process Regression (GPR). The technical details will be light regarding all decisions made in the application of this approach, and only the equations necessary for reproduction of results will be included.

Gaussian-Process Regression can be seen as a direct extension of the standard linear regression which is commonly used in engineering practice. While possible with standard linear regression, GPR places much more emphasis on the distribution (representing uncertainty) of the modeled response, i.e. yield in this specific case. The primary

extension is to accomplish "non-parametric regression", meaning it is not limited to any pre-specified basis functions (i.e. no pre-specified model form). Full justification of how to achieve this behavior is provided elsewhere [45, 46], but brief descriptions of two ways of performing GPR are as follows: to assume an autocorrelation function and apply Bayes' law to the jointly normal distributed variables, or to start with standard linear regression and apply the "kernel trick" to an infinite series of wavelet bases. We adopt the Bayesian mentality in which the UQ analysis starts from a state of prior knowledge then incorporates the data at hand to a posterior state of knowledge.

Since the yield X is function of the particle temperature T, we assumed the following squared-exponential autocorrelation function, o covariance kernel:

$$K^{(\text{s.e.})}(T_a, T_b) = \sigma^2 \exp\left(-\left(\frac{T_a - T_b}{\ell_{\text{corr}}}\right)^2\right), \tag{8}$$

where T_a and T_b are two randomly-selected temperatures, coming either from the data points or the inference points, σ^2 is the (uncertain) maximum covariance and ℓ_{corr} is the (uncertain) correlation length-scale. The latter defines how much observations at temperature T_a will have negligible effect in the interpolation of the yield at new T_b values.

Bayesian methods are most commonly used with rather uninformative priors, other than the structure of the statistical model. However, for small data sets any relevant prior data is highly desirable since it can significantly improve the posterior approximation. Care must be taken here, to limit the claim of prior information only to what is known with relative certainty. In this spirit, the study was limited to the following prior information:

- Having reached steady state on a geological timescale, the yield must be zero, with zero gradient, at the underground temperature. For the purpose of this study 300 K was selected as representative temperature. The analysis is easily recalculated with any smaller value.
- Considering the boiling point of graphite to be ∼3800 K [47] (graphite representing the strongest bond types within the coal/char), the yield must be unity at this temperature.

Other than these two facts, the prior mean function μ and the prior covariance magnitude σ^2 were selected to remain quite uninformative, resulting in a wide multivariate Gaussian distribution. On whole, we characterize the prior for yield to be "weakly informative". A standard GPR approach results in a posterior distribution of the form

$$X|X_d \sim \mathcal{N}\left(K_{id}K_{dd}^{-1}(X_d - \mu_d) + \mu_i,\, K_{ii} - K_{id}K_{dd}^{-1}K_{di}\right), \tag{9}$$

where μ represents prior means (subscripts d & i representing data points and inference points respectively), K represents covariances calculated from a kernel and $X|X_d$ represents the conditioning of the data points X_d on the prediction X. The selected kernel can have two contributions, squared-exponential and noise, which together result in the non-parametric regression. The explicit form of squared-exponential kernel is shown in Eq. 8. Since our intended inference is a noise-free underlying process, the squared-exponential kernel is sufficient for all covariances at inference points ($K = K^{(\text{s.e.})}$, for K_{ii}, K_{id}, & K_{di}), while for measurements the noise kernel $K^{(\text{n.})}$ is included, i.e. $K = K^{(\text{s.e.})} + K^{(\text{n.})}$ for K_{dd} only. The noise kernel is:

$$K^{(\text{n.})} = \varepsilon^2 \delta(T_a, T_b), \tag{10}$$

with ε representing the uncertain experimental noise, and δ representing the Kronecker function.

A side note is worth making here about the noise parameter ε. The intuitive meaning of the noise is directly reproduced in the mathematics of the posterior in the following way: if $\varepsilon = 0$, then the resulting yield model will exactly reproduce the experimental yield data at each measured temperature. This condition would result in an interpolated yield model rather than a regressed one, and a resulting distribution across yield (at a temperature between measured values) would represent only interpolation error. As the noise parameter is allowed to be larger, the modeled yield is less tightly bound to the measured data values. In this line of reasoning, having repeated data of yield at a single temperature (or close-by temperatures) provides significant information about the magnitude of the experimental noise.

For determination of these remaining uncertain parameters, ℓ_{corr} and ε, the standard GPR approach provides the joint posterior:

$$\begin{aligned} \ln\left(p(\ell_{\text{corr}}, \varepsilon | X_d)\right) = &-\tfrac{1}{2}(X_d - \mu_d)^\intercal K_{dd}^{-1}(X_d - \mu_d) \\ &-\tfrac{1}{2}\ln(\det(K_{dd})) + \ln(p_0) + C, \end{aligned} \tag{11}$$

where p_0 is the prior for the parameters (constant when uninformative) and C is an unimportant normalizing constant [25]. Finally, the method simultaneously provides an estimate for the experimental noise, an estimate for the underlying yield curve (as a function of temperature), and an estimate for a correlation length-scale of yield across temperature. Only one modification of the standard approach was required in this study. The data of interest did not represent the measurement of a single particle yield at a single temperature. Rather, it represented the measurement of one collective yield for a population of particles having a temperature distribution. For a simple, known particle distribution this complication could be incorporated into the Bayesian methodology simply by analytical convolution of the data kernel. In this case, a more complex distribution was determined through numerical simulation, and applied as a linear operation to the kernel as a filter. This is accomplished by listing the particle temperatures (or binning then into a histogram, as done in Fig. 2), constructing a prior mean, μ_p and covariances, K_{di}, K_{id}, & K_{pp} (all using the squared-exponential kernel), at these individual particle locations (or bin locations). Next, one should construct a weight matrix, W, that represents the contribution of each particle (or bin) to each measurement datum. This results in a shape of the weight matrix as: the total number of particles by the number of data measurements. Then the filter is applied accordingly and the results are discussed in Section 6.

6. Results

6.1. Consistency

The analysis presented in Section 5.1 was performed on the BT model (Eq. 3) and an inconsistent dataset was found, even though a maximum relative error of 50% for all the data was considered. Figure 4 shows representative yield curves predicted by the BT model with values of parameters DI and T_{st} changing in the range [0.1,0.9] and [800,1600], respectively. None of the predicted curves overlap with all the experimental data.

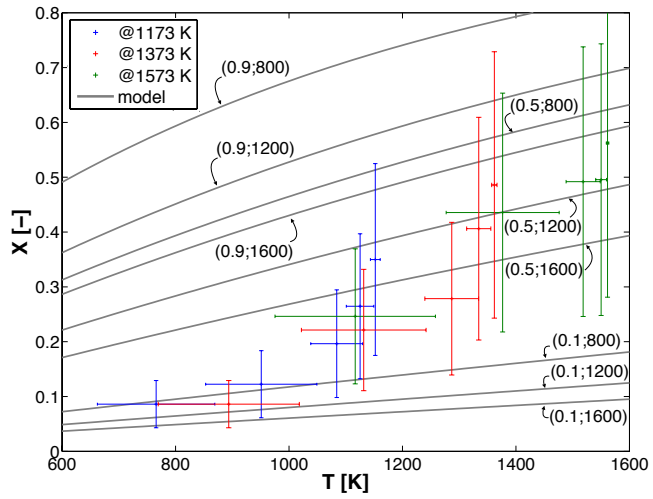

Figure 4: Experimental data with 50% relative error on conversion values and nine representative yield curves predicted by the BT model (Eq. 3) with values of parameters DI and T_{st} changing in the range [0.1,0.9] and [800,1600], respectively. Each pair of values indicates DI (first number) and T_{st} (second number) at which the corresponding curve has been obtained. The data provided by the same test are grouped with the same color. Horizontal bars represent the particle temperature interval at each sampling point, determined by CFD analysis.

The analysis presented in Section 5.1 was then performed on the new yield model (Eq. 7) and a consistent dataset was found considering a relative error of 18% for all the data. The consistent space for the yield model parameters T_1 and T_2 is shown in Fig. 5. Figure 6 shows the data, with the updated error, at the different temperatures and the model curves predicted by the yield model using all the consistent values of parameters T_1 and T_2.

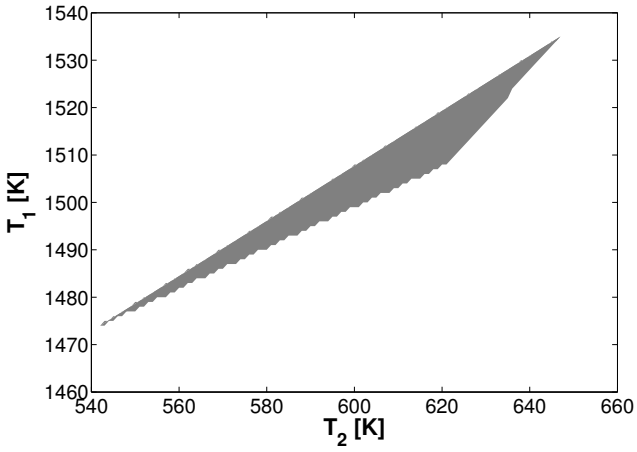

Figure 5: Consistent region of the yield model parameters T_1 and T_2.

6.2. GPR

The posterior for yield obtained with the method discussed in Section 5.2 is shown in Fig. 7, along with the experimental data. Figure 7 shows the reduction of uncertainty relative to the prior as obtained from the GPR approach. The method is able to empirically indicate potential model forms that could be explored in the future to account for uncertainty in the yields, especially at higher temperatures. Additionally a joint posterior distribution

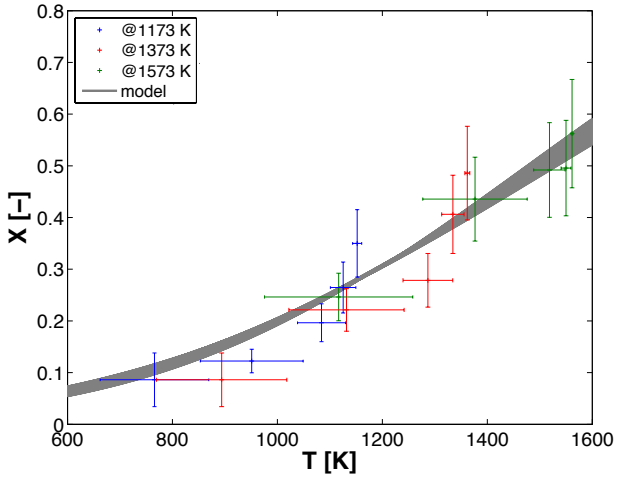

Figure 6: Experimental data with 18% relative error on conversion values and yield curve predicted by the yield model (Eq. 7) with consistent values of parameters T_1 and T_2. The data provided by the same test are grouped with the same color. Horizontal bars represent the particle temperature interval at each sampling point, determined by CFD analysis.

was obtained for the parameters ε and ℓ_{corr}. This posterior was sufficiently narrow, that the maximum-likelihood estimate was considered sufficiently accurate for these two parameters. The posterior mode was located at: $\varepsilon = 0.058$ and $\ell_{\text{corr}} = 677$ K. Until data is available in such temperature regions, it will be difficult to compare potential model forms and reach definitive conclusions. Even if experimental data of pure devolatilization does not become available in the near future, model forms such as those suggested could be tested within multi-physics simulations against data forms available for comparison at that scale. The boiling point of graphite, nominally ~3800 K, has significant uncertainty, due to insufficient experimental data as well as due to varying sheet size or the presence of imperfections. The statistical analysis was repeated while varying the graphite boiling temperature by +/- 400 K. The resulting posterior, in the temperature range of industrial interest, changed only negligibly.

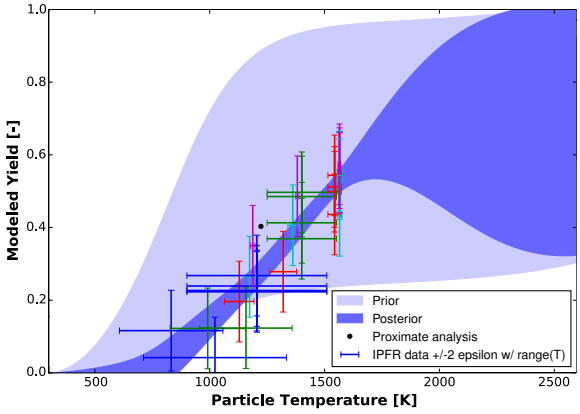

Figure 7: Prior credible interval, 95% (light shaded area), posterior credible interval, 95% (dark shaded area), for yield and experimental data (horizontal bars, range of particle temperatures & vertical bars, experimental noise $\pm 2\varepsilon$) from IPFR. The different colors of experimental data account for the five different sampling points, as in Fig. 2.

The obtained posterior yield is subsequently compared with the yield curves provided by the models presented in this work, see Fig. 8. As proved by the numerical simulations presented in Section 3, the BT models fail in the prediction of the particle conversion achieved at different heights of the IPFR. BT can be considered as a possible model form only for temperatures above 1500 K. More experimental data are necessary to shed lights on the devolatilization behaviour of coal particles at temperatures higher than about 1750 K, where the reduction of uncertainty is not achieved.

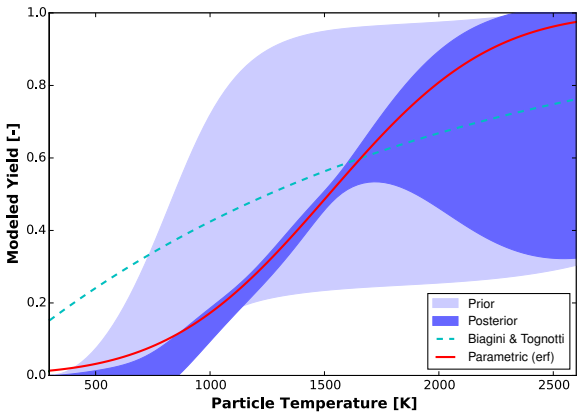

Figure 8: Prior credible interval, 95%, (light shaded area) and empirical posterior credible interval, 95%, of the yield (dark shaded area), yield curve explicitly provided by the BT model (dashed curve), and a proposed yield curve (solid line).

Two important observations should be noted regarding the validity of the two approaches:

- the experimental error estimates found with the two methods are of the same order of magnitude: a 18% relative error was required to ensure consistency of the new yield model, while the posterior sigma ensuring 95% confidence interval on data (2ε) is equal to 12%;
- the function evaluated through the consistency analysis is included within the posterior derived from GPR, indicating that it can satisfactorily match the experimental data and provide reliable estimation in almost every range of temperatures.

6.3. Final validation

The novel yield model shown in Eq. 7, with consistent parameters found through the methodology described in Section 5.1, fits the posterior model form outlined by the GPR approach. The model was implemented in Fluent, a fast first-order kinetics was set in order to allow the particles to reach the equilibrium, and the results are shown in Fig. 9.

The results are satisfactory for all the experimental cases. The conversion values at residence times higher than 0.15 s, when the particles reach the nominal reactor temperatures, are well estimated. An underprediction of particle conversion can be noticed at residence times lower than 0.05 s, at 1173 K and 1373 K, indicating that the presence of a kinetically limited regime can be hypothesized where the particle temperature is still below 1000 K.

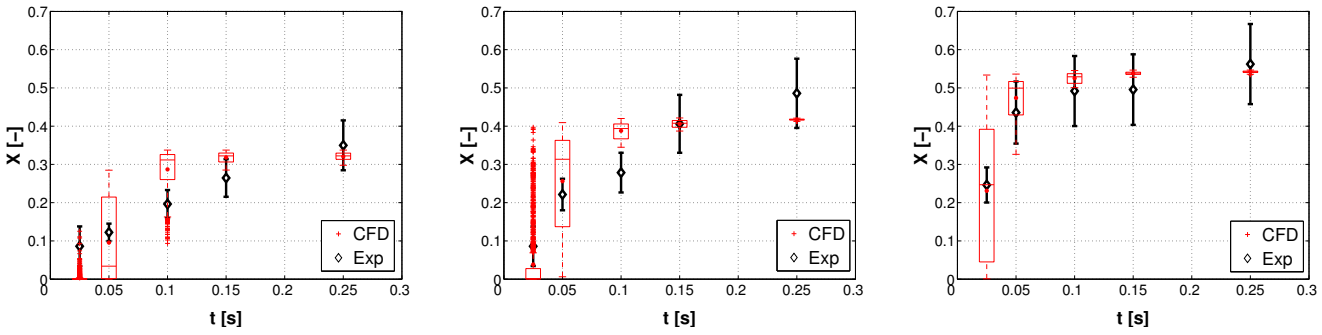

Figure 9: Boxplots of particle conversions vs. residence times for the novel yield model at 1173 K (a), 1373 K (b) and 1573 K (c).

7. Conclusion

Two methodologies based on joint experimental and numerical investigations of coal devolatilization were used to propose a new yield model, for application in large-scale CFD simulations. The approach was demonstrated for the devolatilization of Sebuku bituminous coal in oxy-coal conditions, in the IFRF's entrained flow reactor. Preliminary CFD simulations in inert conditions provided the particle thermal histories, which were not measured during the experiments. An analysis of the temperatures reached by the particles inside the facility led to the assumption that chemical equilibrium occurs at the highest residence times and temperatures. CFD simulations with an empirical (BT) devolatilization model, which includes a yield model, were then performed to identify the limitations of the model in the prediction of coal conversion for conditions where equilibrium is reached. The BT model partially failed to predict the particle conversion, and a procedure to improve the model performances was then required. The uncertainty affecting the BT model parameters has been investigated using a consistency analysis performed on the overall available dataset, i.e. the union of the experimental data, the uncertainty in the measurement and the additional information provided by numerical simulations. The attempt to tweak the BT model through its parameters was unsuccessful, raising the issue of the presence of model form uncertainty, i.e. the uncertainty that exists in the process of selecting the best model from a model set.

A Gaussian-Process Regression was performed, to improve the understanding of the uncertainty associated to the coal devolatilization process, based on the available experimental measurements. A posterior state of knowledge, indicating potential model forms that could be explored in yield modeling, was obtained. Thus, a possible reduced physics model for the coal yield has been proposed, based on only two parameters which were once again calibrated using a consistency analysis against the selected quantity of interest of the problem, i.e. the conversion or yield. The dataset was found consistent when a relative error of 18% for all the data was applied, and the consistent space of the model parameters was provided. The model form evaluated through the consistency analysis is included within the posterior derived from GPR, indicating that it can satisfactorily match the experimental data and provide reliable estimation in almost every range of temperatures.

Once the model form and experimental uncertainties had been quantified with the two methods, CFD simulations were carried out using the novel ultimate yield model with first-order kinetics. Results show promising agreement between predicted and experimental conversion for all cases. This work shows an innovative procedure that joins

experiments and simulations to assess both model parameter and model form uncertainty regarding, in this case, the ultimate volatile yield. A yield model can improve the predictivity of reduced physics models for coal devolatilization. The procedure can be simply applied to alternative coal types, to derive scale-bridging models describing both kinetic and thermodynamic aspects, as different model forms can be chosen and evaluated. As model-form uncertainty exists and has been evaluated, also instrument model-form uncertainty subsists and can be assessed. The term "instrument model" refers to all the physical sub-models in both the experimental scenarios and the numerical simulations. The uncertainty associated with the instrument modeling and how it propagates through the process will be further investigated by the authors in their future work.

The process has the potential for continuous refinement, e.g., the inclusion of experimental data provided at temperature higher than 1600 K could greatly reduce the uncertainty in the model form for higher temperature applications, as it has been illustrated through the GPR approach. Moreover, the focus on a large validation dataset will ensure, in a Bayesian perspective, predictivity with uncertainty quantification for a validated model. The procedure described in this work turned out to be useful and valuable for the assessment of the "goodness" of experimental data and the quantification of the sometimes underestimated experimental error, and its strength lies in its applicability for different experimental facilities and scenarios, in a wide range of scales and fields, other than combustion science.

Acknowledgments

This material is based upon work supported by the US Department of Energy, National Nuclear Security Administration, under Award Number(s) DE-NA0002375.

References

[1] E. Smeets, A. Faaij, I. Lewandowski, W. Turkenburg, A bottom-up assessment and review of global bio-energy potentials to 2050, Prog. Energ. Combust. 33 (1) (2007) 56–106. doi:http://dx.doi.org/10.1016/j.pecs.2006.08.001.
URL http://www.sciencedirect.com/science/article/pii/S0360128506000359

[2] J. Katzer, The future of coal: an interdisciplinary MIT study., Tech. rep., Massachusetts Institute of Technology (2007).

[3] T. Wall, Y. Liu, C. Spero, L. Elliott, S. Khare, R. Rathnam, F. Zeenathal, B. Moghtaderi, B. Buhre, C. Sheng, R. Gupta, T. Yamada, K. Makino, J. Yu, An overview on oxyfuel coal combustion—state of the art research and technology development, Chem. Eng. Res. Des. 87 (8) (2009) 1003–1016. doi:http://dx.doi.org/10.1016/j.cherd.2009.02.005.
URL http://www.sciencedirect.com/science/article/pii/S0263876209000598

[4] L. Álvarez, M. Gharebaghi, J. M. Jones, M. Pourkashanian, A. Williams, J. Riaza, C. Pevida, J. J. Pis, F. Rubiera, CFD modeling of oxy-coal combustion: Prediction of burnout, volatile and no precursors release, Appl. Energ. 104 (2013) 653–665. doi:http://dx.doi.org/10.1016/j.apenergy.2012.11.058.
URL http://www.sciencedirect.com/science/article/pii/S030626191200863X

[5] M. Rabaçal, B. Franchetti, F. C. Marincola, F. Proch, M. Costa, C. Hasse, A. Kempf, Large Eddy Simulation of coal combustion in a large-scale laboratory furnace, Proc. Combust. Inst. 35 (3) (2015) 3609–3617.

[6] D. B. Anthony, J. B. Howard, Coal devolatilization and hydrogastification, AIChE J. 22 (4) (1976) 625–656. doi:10.1002/aic.690220403.
URL http://dx.doi.org/10.1002/aic.690220403

[7] H. Kobayashi, J. Howard, A. Sarofim, Coal devolatilization at high temperatures, Symp. (Int.) Combust. 16 (1) (1977) 411–425. doi:http://dx.doi.org/10.1016/S0082-0784(77)80341-X.
URL http://www.sciencedirect.com/science/article/pii/S008207847780341X

[8] S. Sommariva, T. Maffei, G. Migliavacca, T. Faravelli, E. Ranzi, A predictive multi-step kinetic model of coal devolatilization, Fuel 89 (2) (2010) 318–328. doi:http://dx.doi.org/10.1016/j.fuel.2009.07.023.
URL http://www.sciencedirect.com/science/article/pii/S0016236109003548

[9] T. Maffei, A. Frassoldati, A. Cuoci, E. Ranzi, T. Faravelli, Predictive one step kinetic model of coal pyrolysis for CFD applications, Proc. Combust. Inst. 34 (2) (2013) 2401–2410. doi:http://dx.doi.org/10.1016/j.proci.2012.08.006.
URL http://www.sciencedirect.com/science/article/pii/S154074891200377X

[10] S. Niksa, A. R. Kerstein, FLASHCHAIN theory for rapid coal devolatilization kinetics. 1. Formulation, Energ. Fuel. 5 (5) (1991) 647–665. arXiv:http://dx.doi.org/10.1021/ef00029a006, doi:10.1021/ef00029a006.
URL http://dx.doi.org/10.1021/ef00029a006

[11] T. H. Fletcher, A. R. Kerstein, R. J. Pugmire, M. S. Solum, D. M. Grant, Chemical percolation model for devolatilization. 3. Direct use of carbon-13 NMR data to predict effects of coal type, Energ. Fuel. 6 (4) (1992) 414–431. arXiv:http://dx.doi.org/10.1021/ef00034a011, doi:10.1021/ef00034a011.
URL http://dx.doi.org/10.1021/ef00034a011

[12] P. R. Solomon, D. G. Hamblen, M. A. Serio, Z.-Z. Yu, S. Charpenay, A characterization method and model for predicting coal conversion behaviour, Fuel 72 (4) (1993) 469–488. doi:http://dx.doi.org/10.1016/0016-2361(93)90106-C.
URL http://www.sciencedirect.com/science/article/pii/001623619390106C

[13] M. Rieth, A. Clements, M. Rabaçal, F. Proch, O. Stein, A. Kempf, Flamelet LES modeling of coal combustion with detailed devolatilization by directly coupled CPD, Proc. Combust. Inst. 36 (2) (2017) 2181 – 2189. doi:https://doi.org/10.1016/j.proci.2016.06.077.
URL http://www.sciencedirect.com/science/article/pii/S1540748916301353

[14] E. Biagini, L. Tognotti, A generalized correlation for coal devolatilization kinetics at high temperature, Fuel Process. Technol. 126 (2014) 513–520. doi:http://dx.doi.org/10.1016/j.fuproc.2014.06.008.
URL http://www.sciencedirect.com/science/article/pii/S0378382014002458

[15] S. Badzioch, P. G. W. Hawksley, Kinetics of thermal decomposition of pulverized coal particles, Ind. Eng. Chem. Process Des. Dev. 9 (4) (1970) 521–530. arXiv:http://dx.doi.org/10.1021/i260036a005, doi:10.1021/i260036a005.
URL http://dx.doi.org/10.1021/i260036a005

[16] S. Niksa, Predicting the devolatilization behavior of any coal from its ultimate analysis, Combust. Flame 100 (3) (1995) 384–394. doi:http://dx.doi.org/10.1016/0010-2180(94)00060-6.
URL http://www.sciencedirect.com/science/article/pii/0010218094000606

[17] A. K. Burnham, , R. L. Braun, Global kinetic analysis of complex materials, Energ. Fuel. 13 (1) (1999) 1–22. arXiv:http://dx.doi.org/10.1021/ef9800765, doi:10.1021/ef9800765.
URL http://dx.doi.org/10.1021/ef9800765

[18] A. Williams, R. Backreedy, R. Habib, J. Jones, M. Pourkashanian, Modelling coal combustion: the current position, Fuel 81 (5) (2002) 605–618. doi:http://dx.doi.org/10.1016/S0016-2361(01)00158-2.
URL http://www.sciencedirect.com/science/article/pii/S0016236101001582

[19] L. Álvarez, M. Gharebaghi, M. Pourkashanian, A. Williams, J. Riaza, C. Pevida, J. Pis, F. Rubiera, CFD modelling of oxy-coal combustion in an entrained flow reactor, Fuel Process. Technol. 92 (8) (2011) 1489–1497. doi:http://dx.doi.org/10.1016/j.fuproc.2011.03.010.
URL http://www.sciencedirect.com/science/article/pii/S0378382011001020

[20] A. H. Al-Abbas, J. Naser, D. Dodds, CFD modelling of air-fired and oxy-fuel combustion of lignite in a 100 KW furnace, Fuel 90 (5) (2011) 1778–1795. doi:http://dx.doi.org/10.1016/j.fuel.2011.01.014.
URL http://www.sciencedirect.com/science/article/pii/S0016236111000160

[21] Q. Fang, A. A. B. Musa, Y. Wei, Z. Luo, H. Zhou, Numerical simulation of multifuel combustion in a 200 MW tangentially fired utility boiler, Energ. Fuel. 26 (1) (2012) 313–323. arXiv:http://dx.doi.org/10.1021/ef201149p, doi:10.1021/ef201149p.
URL http://dx.doi.org/10.1021/ef201149p

[22] H. Gao, A. Runstedtler, A. Majeski, R. Yandon, K. Zanganeh, A. Shafeen, Reducing the recycle flue gas rate of an oxy-fuel utility power boiler, Fuel 140 (2015) 578–589. doi:http://dx.doi.org/10.1016/j.fuel.2014.09.065.
URL http://www.sciencedirect.com/science/article/pii/S001623611400934X

[23] S. Iavarone, C. Galletti, F. Contino, L. Tognotti, P. J. Smith, A. Parente, Cfd-aided benchmark assessment of coal devolatilization one-step models in oxy-coal combustion conditions, Fuel Process. Technol. 154 (2016) 27–36. doi:http://dx.doi.org/10.1016/j.fuproc.2016.07.013.
URL http://www.sciencedirect.com/science/article/pii/S0378382016303149

[24] R. Feeley, P. Seiler, A. Packard, M. Frenklach, Consistency of a reaction dataset, J. Phys. Chem. A 108 (44) (2004) 9573–9583. arXiv:http://dx.doi.org/10.1021/jp047524w, doi:10.1021/jp047524w.
URL http://dx.doi.org/10.1021/jp047524w

[25] A. Gelman, J. Carlin, H. Stern, D. Dunson, A. Vehtari, D. Rubin, Bayesian Data Analysis, Third Edition, Chapman & Hall/CRC Texts in Statistical Science, 2014.

[26] M. Simone, E. Biagini, C. Galletti, L. Tognotti, Evaluation of global biomass devolatilization kinetics in a drop tube reactor with CFD aided experiments, Fuel 88 (10) (2009) 1818–1827. doi:http://dx.doi.org/10.1016/j.fuel.2009.04.032.
URL http://www.sciencedirect.com/science/article/pii/S0016236109002087

[27] O. Authier, E. Thunin, P. Plion, L. Porcheron, Global kinetic modeling of coal devolatilization in a thermogravimetric balance and drop-tube furnace, Energ. Fuel. 29 (3) (2015) 1461–1468. arXiv:http://dx.doi.org/10.1021/ef502600t, doi:10.1021/ef502600t.
URL http://dx.doi.org/10.1021/ef502600t

[28] M. Schiemann, S. Haarmann, S. Wirtz, V. Scherer, M. Ehmann, C. Kuhr, Combustion characterisation of fuels for power plants: From laboratory experiments to boiler furnace simulation, Tech. rep., VGB PowerTech (2016).

[29] R. Jovanovic, A. Milewska, B. Swiatkowski, A. Goanta, H. Spliethoff, Sensitivity analysis of different devolatilisation models on predicting ignition point position during pulverized coal combustion in O2/N2 and O2/CO2 atmospheres/N2 and O2/CO2 atmospheres and O2/CO2 atmospheres, Fuel 101 (2012) 23–37. doi:http://dx.doi.org/10.1016/j.fuel.2011.02.024.
URL http://www.sciencedirect.com/science/article/pii/S0016236111000949

[30] M. Vascellari, R. Arora, M. Pollack, C. Hasse, Simulation of entrained flow gasification with advanced coal conversion submodels. Part 1: Pyrolysis, Fuel 113 (2013) 654–669. doi:http://dx.doi.org/10.1016/j.fuel.2013.06.014.
URL http://www.sciencedirect.com/science/article/pii/S0016236113005413

[31] C. Galletti, L. Giovannini, G. Coraggio, L. Tognotti, Analysis of oxy-coal combustion through measurements in a pilot-scale entrained flow reactor, Chem. Eng. Trans. 32 (2013) 709–714.

[32] Prime database [cited December 2016].
URL www.primekinetics.org

[33] E. Biagini, L. Biasci, M. Marcucci, Description of the isothermal plug flow reactor and the experimental procedures for combustion studies on solid fuels, Tech. Rep. G03/y/03, IFRF (2010).

[34] E. Biagini, G. Bonvicini, G. Coraggio, M. Faleni, Development of the experimental procedures for advanced biofuels characterization in the isothermal plug flow reactor, Tech. Rep. G27/y/01, IFRF (2013).

[35] E. Biagini, F. Barontini, G. Bonvicini, G. Coraggio, L. Tognotti, Advanced characterization of biofuels for combustion and gasification plants, Chem. Eng. Trans. 37 (2014) 493–498. doi:10.3303/CET1437083.
URL http://www.scopus.com/inward/record.url?eid=2-s2.0-84899413621&partnerID=40&md5=d2f9af3defa92894654369601ccf83e5

[36] G. Bonvicini, G. Coraggio, M. Faleni, Coal characterization in oxy-firing conditions using the isothermal plug flow reactor. part 1 – methodology, Tech. Rep. G26/y/01, IFRF (2013).

[37] G. Bonvicini, G. Coraggio, M. Faleni, Coal characterization in oxy-firing conditions using the isothermal plug flow reactor. part 2 – experimental results, Tech. Rep. F112/y/01, IFRF (2013).

[38] D. Anthony, J. Howard, H. Hottel, H. Meissner, Rapid devolatilization of pulverized coal, Symp. (Int.) Combust. 15 (1) (1975) 1303–1317. doi:http://dx.doi.org/10.1016/S0082-0784(75)80392-4.
URL http://www.sciencedirect.com/science/article/pii/S0082078475803924

[39] J. Yu, J. A. Lucas, T. F. Wall, Formation of the structure of chars during devolatilization of pulverized coal and its thermoproperties: A review, Prog. Energ. Combust. 33 (2) (2007) 135–170. doi:http://dx.doi.org/10.1016/j.pecs.2006.07.003.
URL http://www.sciencedirect.com/science/article/pii/S0360128506000372

[40] N. Hashimoto, R. Kurose, S.-M. Hwang, H. Tsuji, H. Shirai, A numerical simulation of pulverized coal combustion employing a tabulated-devolatilization-process model (tdp model), Combust. Flame 159 (1) (2012) 353–366. doi:http://dx.doi.org/10.1016/j.combustflame.2011.05.024.
URL http://www.sciencedirect.com/science/article/pii/S0010218011001702

[41] Solid fuel database [cited December 2016].
URL http://sfdb.ifrf.net/

[42] M. Frenklach, A. Packard, P. Seiler, Prediction uncertainty from models and data, in: Proceedings of the American Control Conference, Vol. 5, 2002, pp. 4135–4140. doi:10.1109/ACC.2002.1024578.

[43] M. Frenklach, A. Packard, P. Seiler, R. Feeley, Collaborative data processing in developing predictive models of complex reaction systems, Int. J. Chem. Kinet. 36 (1) (2004) 57–66. doi:10.1002/kin.10172.
URL http://dx.doi.org/10.1002/kin.10172

[44] C. Please, M. McGuinness, D. McElwain, Approximations to the distributed activation energy model for the pyrolysis of coal, Combust. Flame 133 (1-2) (2003) 107–117. doi:http://dx.doi.org/10.1016/S0010-2180(02)00554-0.
URL http://www.sciencedirect.com/science/article/pii/S0010218002005540

[45] M. Ebden, Gaussian processes: A quick introduction (2015) [cited 24 November 2016].
URL http://arxiv.org/abs/1505.02965v2

[46] E. Snelson, Flexible and efficient gaussian process models for machine learning, Ph.D. thesis, Gatsby Computational Neuroscience Unit, University College London (2007).

[47] A. Savvatimskiy, Carbon at High Temperatures, Springer Series in Materials Science, Springer, 2015.